Transparent Conductive Oxide Layer and Hole Selective Layer Free Back-Contacted Hybrid Perovskite Solar Cell

Transparent Conductive Oxide Layer and Hole Selective Layer Free Back-Contacted Hybrid Perovskite Solar Cell

Zhaosheng Hu [+], *Gaurav Kapil* [+], *Hiromitsu Shimazaki*[+], *Shyam Sudhir Pandey*[+], *Tingli Ma*[+], *and Shuzi Hayase*[+]*

[+] Graduate School of Life Science and Systems Engineering, Kyushu Institute of Technology. 2-4 Hibikino, Wakamatsu-ku, Kitakyushu 808-0196, Japan

[*] Corresponding author E-mail addresses: hayase@life.kyutech.ac.jp

Abstract

Back-contacted architectures have been under intensive investigation for that transparent conductive oxide (TCO) free can be easily realized which avoids the transmission loss of light caused by TCO, typically comprised in conventional solar cells (SCs). Here, network-like porous Ti was firstly utilized as the back-contacted electrode and a new design allows for a novel back-contacted hybrid perovskite SC without TCO and hole selective layer, which shows a power output of 3.88% with long-term stability. In addition, it avoids limit available collection area of electrodes in the recent reported interdigitated electrode (IDE) based back-contacted TCO-less SCs.

1. Introduction

Recent years have witnessed that hybrid perovskite (PVK) solar cells (SCs) have been identified as one of the most promising solar cells because of the high photoconversion efficiencies[1-4]. In the conventional perovskite SCs, transparent conductive oxide layer (TCO) is typically needed. However, the TCO layer needs complex equipment and process but also leads to hampered incident light on the active layer while passing though the TCO layer. In order to provide an amicable solution for these issues, a back-contacted device[5-7] architecture has been reported for the silicon-based solar cells[8,9] and dye-sensitized solar cells[10-12]. In these proposed device architectures, both of the electrodes are located at the same side of the light absorber layer. Back-contacted PVK solar cells with quasi-interdigitated electrode (QIDE) have been recently reported having the photoconversion efficiency of 3.2%[13]. However, the adopted fabrication process includes photolithographic technology which one of the bottle-necks for the large scale production. In addition, hole selective layers (HSL) such as Spiro-OMeTAD(N^2,N^2,$N^{2'}$,$N^{2'}$,N^7,N^7,$N^{7'}$,$N^{7'}$-octakis(4-methoxyphenyl)-9,9′-spirobi[9H-fluorene]-2,2′,7,7′-tetramine), PTAA(Poly(bis(4-phenyl)(2,,4,6-trymethylphenyl)amine) and PEDOT:PSS(poly(3,4-ethylene dioxythiophene):poly(styrene sulfonate) typically comprised in PVK SCs are costly and unstable[14]. Here, we present a novel back-contacted perovskite (PVK) SCs without TCO and HSL.

2. Experimental Section

TCO & HSL free back-contacted hybrid perovskite SCs are composed of glass/mesoporous-TiO_2 &PVK/porous-Ti with native oxide&PVK/mesoporous

ZrO_2&PVK/gold. **Figure 1** shows the schematic fabrication processes in detail. About 1 μm thick mesoporous TiO_2 layer (particle diameter: 250 nm) was deposited by spin-coating on a glass substrate (**Figure 1i**) and successively sintered at 500^0C for 1.3h (**Figure 1ii**). After that, network-like porous Ti (30nm-80nm thickness) was fabricated by sputtering (CFS-4EP-LL, Shibaura Mechatronics) with 250W power and Ti target in Ar atmosphere at room temperature with 5nm/min rate. Here, on the non TiO_2 area, normal compact Ti layer was formed. (**Figure 1iii**) demonstrated the importance selection of rather larger 250nm diameter of TiO_2 for fabricating network-like porous Ti layer. During this step, a thin native oxide layer (compact TiO_2) was automatically formed on the Ti surface.

Then a mesoporous ZrO_2 layer with thickness of about 150 nm (particle diameter: 30 nm) was spin-coated (**Figure 1iv**) and annealed at 400^0C (**Figure 1v**) for 1h-2h. This annealing step not only led to annealing of ZrO_2 but also formed the thermally oxidized Ti to increase the thickness of the compact native oxide layer on the surface of Ti metal. The temperature we adopted is below the melting point of Nano Ti layer to aovid the completely evaporation of the Ti layer. And it maintain a good oxidation effect[15]. Two-step spin-coating method was adopted for the preparation of $CH_3NH_3PbI_3$ perovskite layer (**Figure 1vi**). First, 460 mg of PbI_2 in 1 ml N,N-dimethylformamide (DMF) and 500 mg of CH_3NH_3I (MAI) in 60 ml isopropanol (IPA) were prepared and kept at 70^0C and room temperature, respectively. This sequential two step deposition method has been reported for the preparation of PVK crystals giving the high photovoltaic performance[16,17]. Samples were prepared by first spin-coating from PbI_2 solution (500 rpm for 5s, followed by 6000 rpm for 10s) and then kept at 70^0C for 30 min. It is worth to mention here that in

the beginning after application of 80µl PbI_2 solution, it was allowed for 1 min of waiting in order to give enough time for spreading of PbI_2 solution over triple porous layers. PbI_2 coated samples were then immerged in MAI solution for 30s for the completely reaction with PbI_2, and then quickly immerged in IPA for 20s to remove the remaining MAI. To complete the device fabrication, 100 nm thick gold was finally deposited by thermal evaporation. Solar cell performances were evaluated using a solar simulator (CEP-2000SRR, Bunkoukeiki Inc., AM 1.5G 100 $mWcm^{-2}$) and a black mask on top of the devices with exposure area 0.12 cm^2 was always used during the photovoltaic measurements.

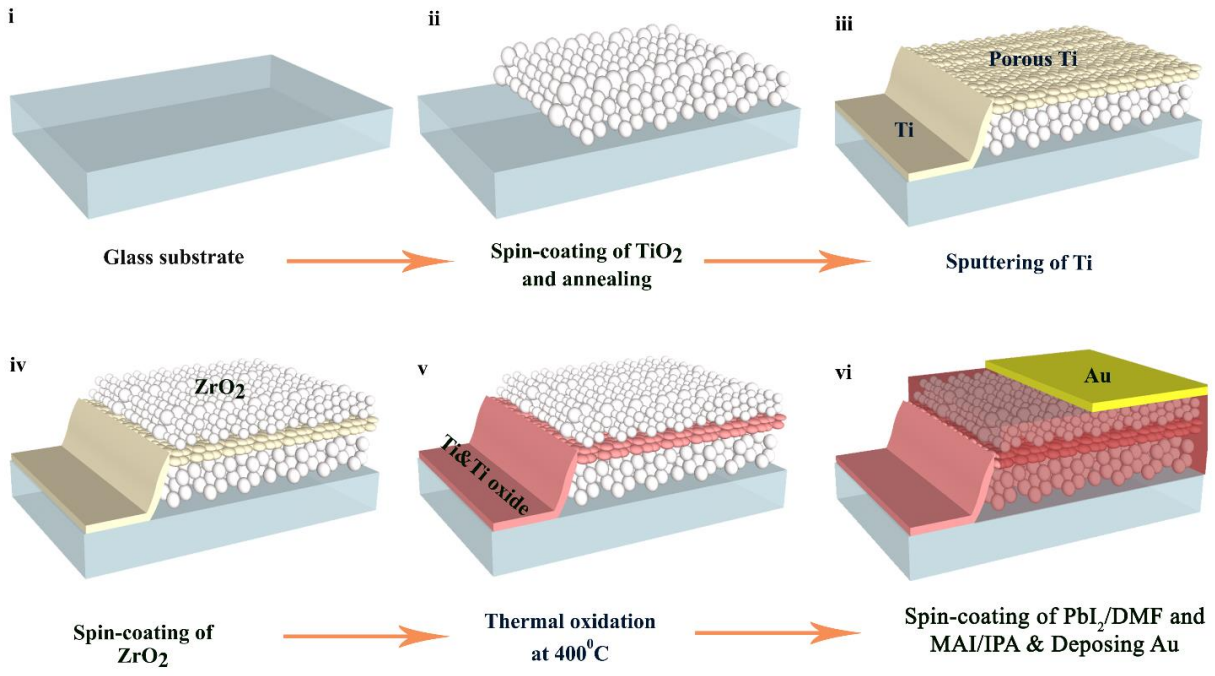

Figure 1 Schematic of fabrication process of TCO & HSL free back-contacted hybrid perovskite solar cell.

3. Results and discussion

Figure 2a shows the architecture of TCO&HSL free back-contacted hybrid perovskite SCs. In this architecture, light comes from the glass side and is absorbed by PVK filled in TiO_2 layer (**Figure 2a iii**). Both electrodes Ti and gold are in the same side of the absorber layer. TCO typically comprised in the sandwich structure of conventional PVK SCs (**Figure 2b**), which is no more necessary in back-contacted structures,[10,11] is omitted. It avoids the transmission loss caused by TCO. Electrodes located in two separated layers have more available collection areas than the IDE based back-contacted SCs, in which two sets of electrodes are narrowed in one layer. Network-like porous Ti (**Figure 2a ii**) is utilized as the back-contacted electrode near the absorber layer because Ti and native oxide on the surface can selectively collect electrons while the generated hole-carriers are available to diffuse in the PVK filled inside the porous and collected by gold electrode. In order to isolate two electrodes, mesoporous ZrO_2 (**Figure 2a i**) is inserted between them, which can effectively avoid the short cut pathway.

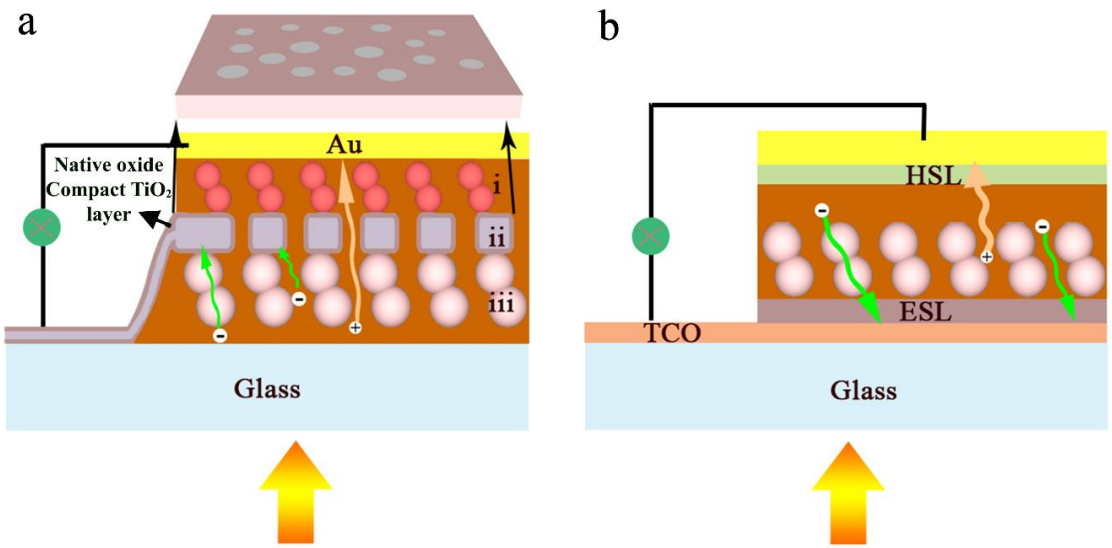

Figure 2 (a) Schematic of TCO & HSL free back-contacted hybrid perovskite solar cell. In the structure, layer i ,ii and iii are mesoporous ZrO_2 filled with PVK, network-like porous Ti with native oxide filled with PVK, mesoporous TiO_2 filled with PVK, respectively. (b) Schematic of conventional PVK solar cell.

Figure 3 shows the carrier collection mechanism on energy diagram. The conduction bands of PVK, compact native oxide layer on Ti (compact TiO_2), and Ti are -3.9 eV, -4.0 eV, -4.3 eV, respectively, forming a smooth electron transfer interface. Since PVK fills nanopores of consecutively fabricated TiO_2 layer, Ti layer and ZrO_2 layer, photogenerated holes diffuse in the PVK filling these triple porous layer, and are finally collected by Au electrode. In addition, holes are kicked out from the porous Ti electrode surface because of the deeper valence band (-7.2 eV) of TiO_2 than that of PVK, and are selectively collected by Au electrode.

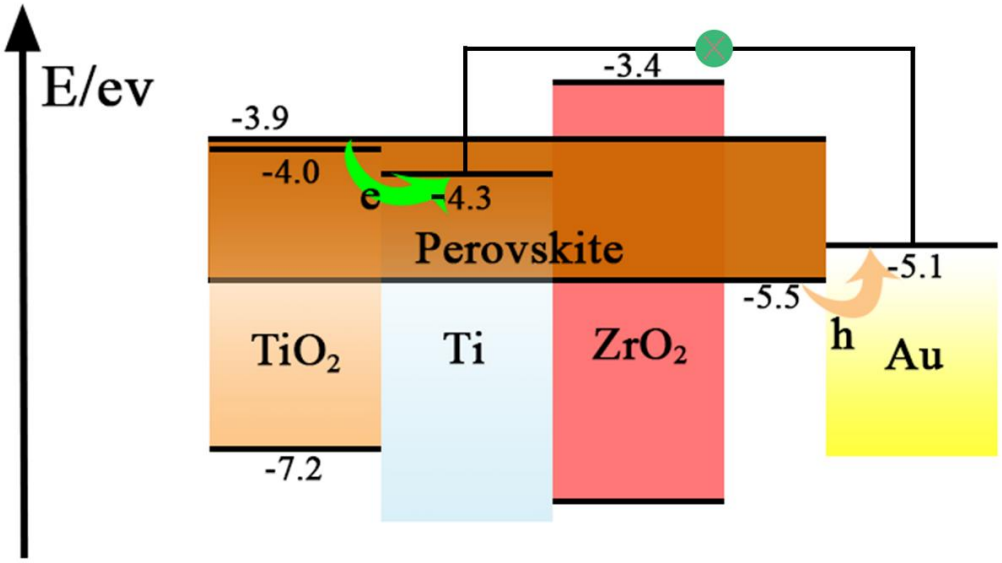

Figure 3 Band diagram of the TCO&HSL free back-contacted hybrid perovskite SC. Energies are expressed in electron volts from vacuum level.

The holes and electrons diffuse in the same direction as shown in **Figure 2**. Therefore, there is possibility of the enhanced recombination of these carriers in this device architecture. Therefore, the whole architecture is very important, especially the structure of back-contacted electrode, which has a sufficient influence on the collection and separation of carriers. The scanning electron microscopic (SEM) images (**Figure 4**) shows that this network-like porous Ti possesses about 250 nm gaps (**Figure 4a and Figure 4b**), which is quite suitable, considering electron diffusion length of 1 micron. The interconnected Ti structure enable high conductivity for collecting electrons. In addition, the interconnected Ti structure can keep the pass of PVK (**Figure 4d**) for carrying holes. Furthermore, compared to the preparation of TCO, the involved

fabrication method, which utilize isotropic deposition of high power pulsed magnetron sputtering on relative large TiO2 (Dimension: 250nm),[18,19] is very simple.

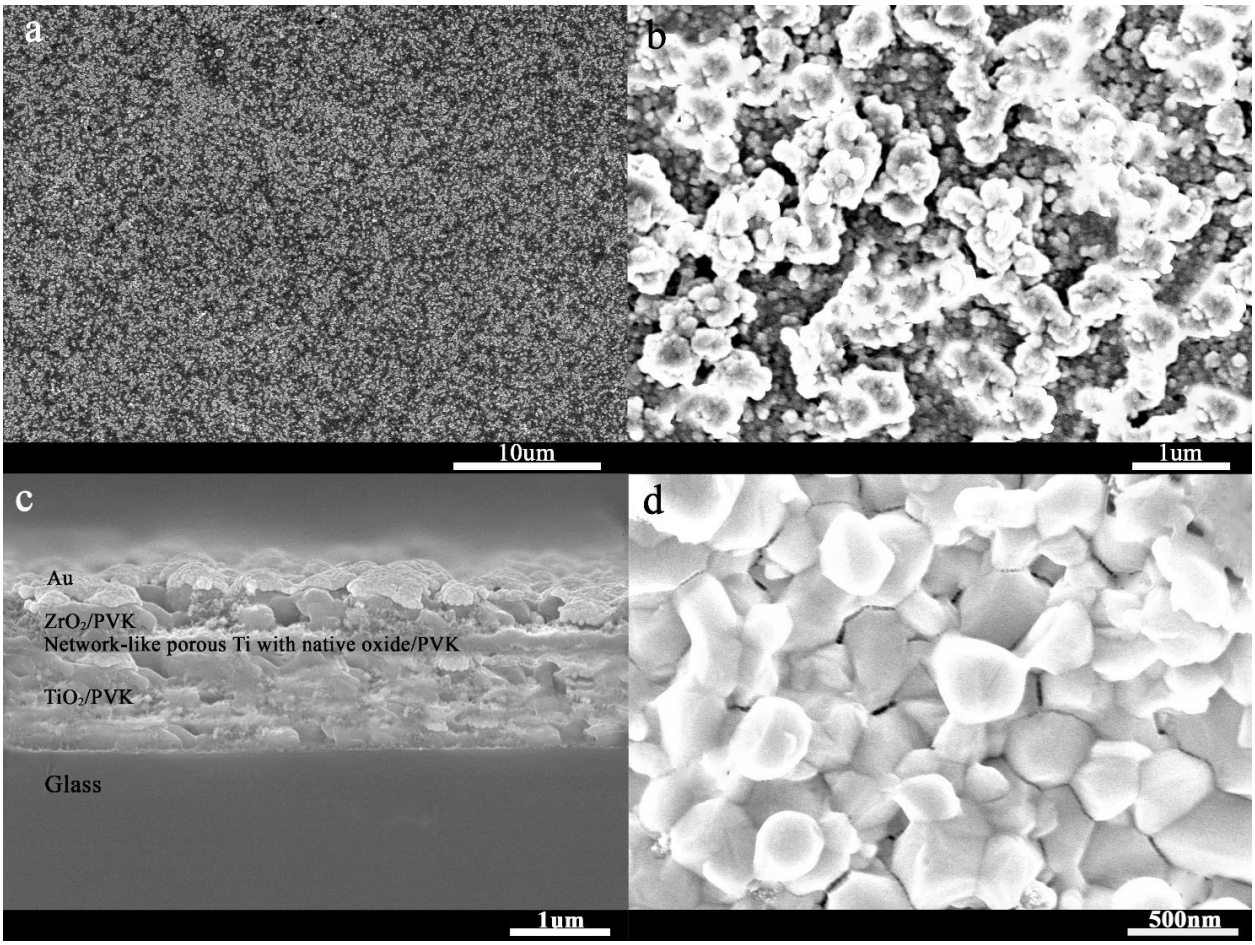

Figure 4 (a) SEM image of network-like porous Ti on porous TiO_2 layer (diameter: 250nm), (b) Expanded SEM image of network-like porous Ti on porous TiO_2. In the SEM image of porous Ti fabricated on porous titania layer (top view), porous titania particles can be seen in the area uncovered by networked Ti. (c) Cross section SEM image of TCO & HSL free back-contacted perovskite SCs including triple mesoporous layers filled with PVK and (d) Top view SEM image of perovskite on ZrO_2/PVK layer.

The SEM cross-section of the complete device (**Figure 4c**) shows four obvious layers including 1 µm TiO_2, 30 nm-80 nm Ti and 150 nm ZrO_2 porous layers. Total thickness of this triple porous layers is about 1.2 µm. The maximum length of the generated hole-carriers diffusing to gold electrode are, therefore, in the same range of the reported diffusion length in perovskites which ensure the facile diffusion of hole-carriers[20-23]. In the back contacted solar cells, sheet resistance plays a crucial role for efficient charge collection. Sheet resistance measured by the four point probe method (**Figure 5a**) indicates that sheet resistance decrease with increasing thickness and saturates after 60 nm thickness having sheet resistance of 11 ohms/sq.

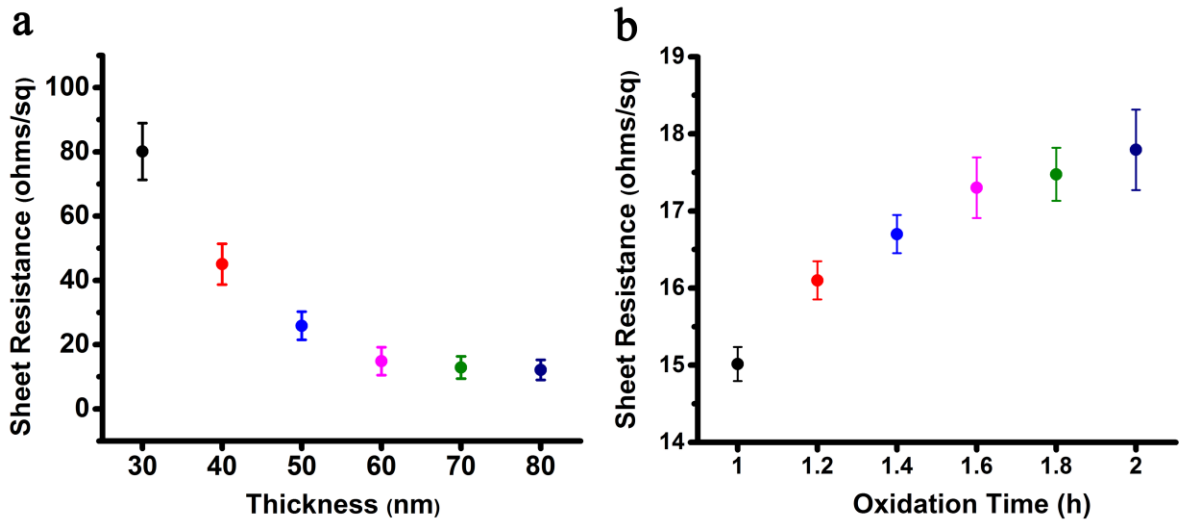

Figure 5 (a) Dependence of the thickness on the sheet resistance of Porous Ti layer on porous TiO_2 layer. (b) Dependence of baking time on the statistical sheet resistance of network-like porous Ti with 60nm thickness on porous TiO_2 layer.

As shown in **Figure 2** and **Figure 3**, light is introduced from TiO_2 (**Figure 6**) side. The porous TiO_2 does not have more light absorption in the area longer than 400nm compared

to the reported TiO_2 (size: 30nm). The large size (250 nm diameter) of TiO_2 nanoparticles in the porous TiO_2 layer scatters light (about 20-25 % reflectance) as shown in **Figure 6**, which works as light confinement layer.

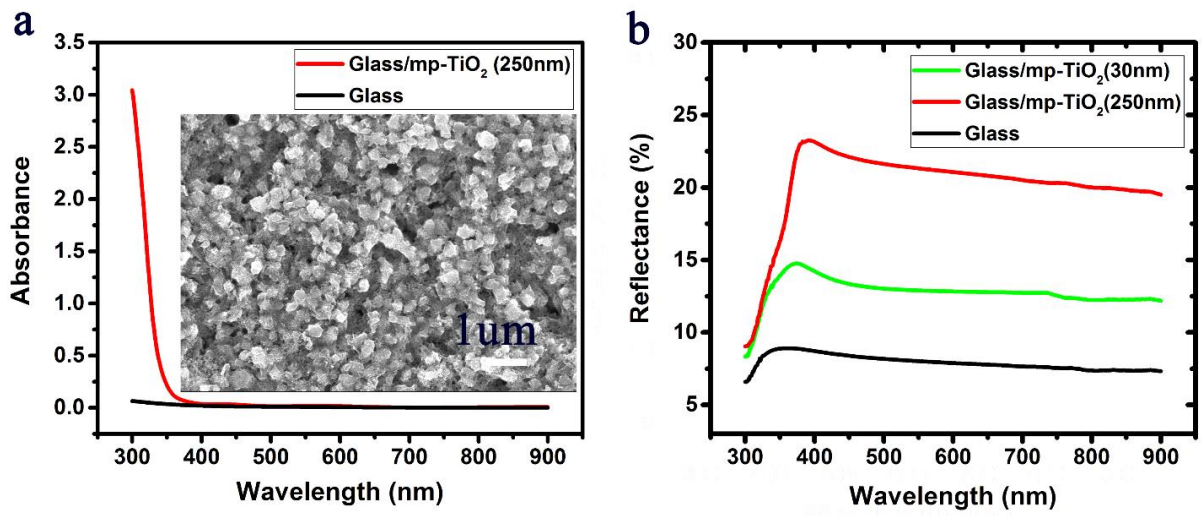

Figure 6 (a) Light absorption and (b) reflectance spectrum of mesoporous TiO2 (250nm) on glass.

The native TiO_2 layer fabricated on Ti by thermal treatment is necessary for suppressing charge recombination. The baking conditions also affect the resistivity (**Figure 5b**). The resistivity increased as the baking time became longer. The slow increase of the rate of the sheet resistance of the Ti electrode with the increasing oxidation time after 1.6 h indicates that Ti surface is almost completely covered with oxide layer. Formation of TiO_2 blocking layer on Ti metal is a conflicting issue to decreasing resistivity of Ti metal.

In order to optimize TCO & HSL free back-contacted structure, systematic investigations concerning the Ti thickness and the thermal oxidation time was conducted aiming at their implications on the photovoltaic performances. We measured power

conversion efficiency (PCE), short-circuit current density (Jsc), fill factor (FF) and open-circuit voltage (Voc) four main parameters of performance of SCs respectively. A perusal of the results shown in the **Figure 7** reveals that Ti thickness of 60 nm was optimum giving the highest efficiency. Ti thickness < 60 nm has been found to give drastically hampered efficiency for the electron collection, because of the sharp increase of the sheet resistance of thinner Ti layer (**Figure 5a**). At the same time, thickness >60 nm obviously reduce PCE, FF, Jsc and Voc (**Figure 7c**) because the size of porous gap of thicker Ti layer becomes smaller and more compact, which seriously decreases the amount of filled perovskite crystals and blocks the facile diffusion of hole-carriers[10,11]. Keeping this optimum thickness of 60 nm in mind, thermal oxidation time was also optimized from 1h to 2h (**Figure 7b and Figure 7d**). An obvious changes in the photovoltaic parameters such as efficiency, Jsc, Voc and FF demonstrate that thermal oxidation time is very crucial for controlling the device performance by forming a completely covered compact oxide layer on Ti metal, which is the key factor for selectively collecting electrons. The optimized thermal oxidation time was found to be 1.8 h. Prolonged oxidation resulted in to the thinner Ti metal electrode with higher resistance leading to reduced device performance.

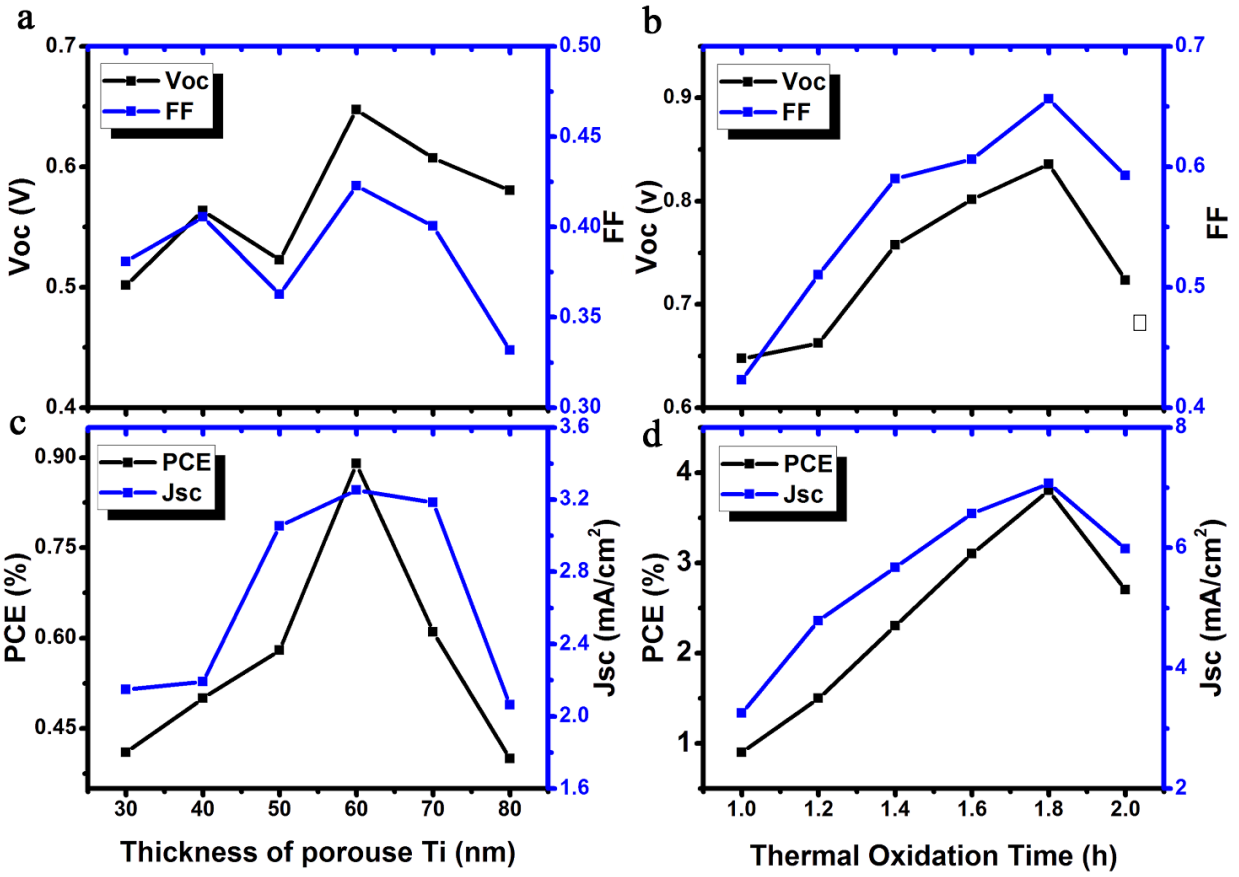

Figure 7 Dependence of thickness of network-like porous Ti upon the photovoltaic parameters such as (a) Voc, FF and (c) PCE, Jsc. Dependence of thermal oxidation time on (b) Voc, FF and (d) PCE, Jsc.

In the case of our newly proposed device structure of TCO & HSL free back-contacted hybrid perovskite SCs having optimized 60 nm thick network-like porous Ti and 1.8 h of thermal oxidation time, J-V characteristics in two scan modes with illumination at 1 Sun shown in the **Figure 8a**. During the measurement, devices were covered with mask with light exposure area of 0.12 cm^2. In forward scan mode (0V → Voc), the values of the Jsc, Voc and FF were found to be 7.07 mA/cm^2, 0.84 V and 0.66, respectively. In reverse scan

mode (Voc → 0V), Jsc, Voc and FF were 7.10 mA/cm^2, 0.83 V and 0.66, respectively. The PCEs of the device in both of the forward as well as reverse scan mode are 3.88 %, which do not show obvious so-called hysteresis phenomenon reported frequently in the perovskite solar cells[24,25].

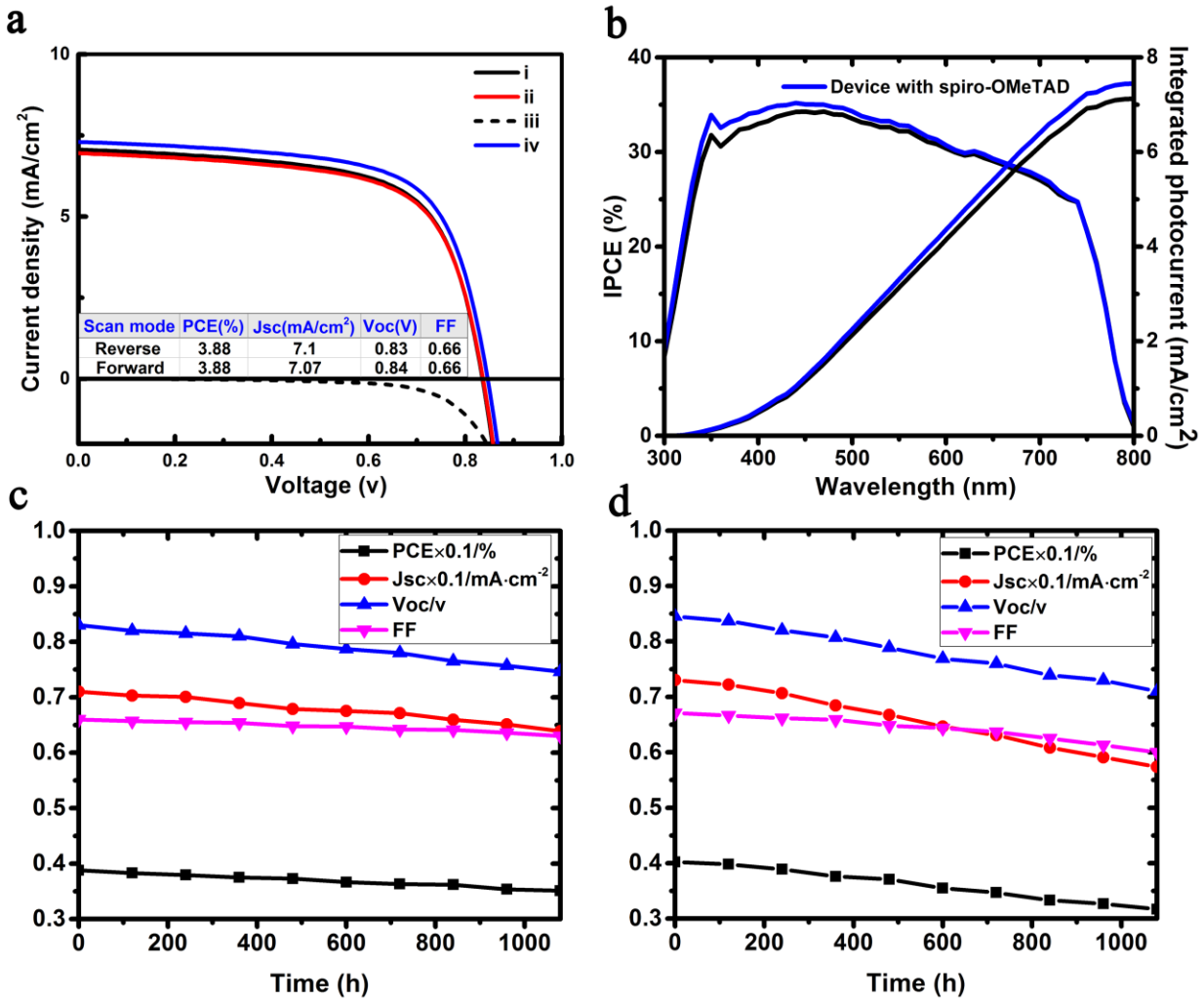

Figure 8 (a) J-V curves of the devices under simulated AM 1.5 solar irradiation measured at room temperature. i) reverse scan, ii) forward scan, iii) dark mode and iv) device with spiro-OMeTAD. (b) IPCE and integrated photocurrent of the devices in the presence and absence of spiro-OMeTAD. Photovoltaic performance change during storage of (c) TCO

and HSL free back-contacted perovskite solar cells and (d) perovskite solar cells with sipro-OMeTAD under light intensity of 100 mW cm^{-2}.

We inserted HTM (spiro-OMeTAD) between mesoporous ZrO_2/PVK and gold electrode to further characterize the separation of generated carriers in ZrO_2 layer. IV in Figure 8a shows the observed PCE of 4.02 % which was a little larger than 3.88% of the device without HTM. A small difference in the photovoltaic performance along with the Incident photon to current conversion efficiency (IPCE) as shown in the **Figure 8b** indicates nearly complete separation of generated carriers in TCO & HSL free back-contacted structure.

Finally, the operational stability were tested under light intensity of 100 mW cm^{-2} in ambient conditions with complete devices without encapsulation. Data is recorded every 120 hours. As shown in **Figure 8c** and **Figure 8d**, in the absence of HTM, the PCE of devices decay 9.6% over 1080 hours show an excellent stability and the devices with Spiro-OMeTAD decay more sharply. This is because of the instability of Spiro-OMeTAD. After 480 hours the performance of the device without HTM even exceed the devices with Spiro-OMeTAD. Under encapsulation, more stable cell performance is expected. Compared to the conventional structure, the performance is still low. One of these reasons may be the relatively higher sheet resistance, 17.5 ohms/sq of network-like porous Ti with oxide on the surface compared to that of around 10 ohms/sq for TCO substrate usually used in solar cells. In addition, the whole path of triple layers structure for hole collections through PVKs filling porous may be too long. Higher efficiency can be expected by optimization the triple layers and replace the Ti with more conductivity

metal (such as Zn), on which oxide layer can be utilized as electron selective layer for perovskite with higher mobility.

4. Conclusion

In conclusion, we have demonstrated a novel back-contacted perovskite solar cell device architecture without using TCO and HSL having PCE of 3.88% under simulated solar irradiation. This architecture avoids the transmission loss caused by TCO, and shows a long-term stability. We have demonstrated the formation of network-like porous Ti electrode. This was accomplished by sputtering Ti on TiO_2 layer with bigger particle size which overcomes the too compact gaps. Furthermore, PVK crystals filled in nanopores in triple porous structure and the native oxide on the network-like porous Ti are very important for collection and separation of carriers. Effect of Ti thickness and thermal oxidation time on the performance of SCs indicated that the completely covered compact native oxide on Ti is crucial for the reduction of charge recombination between electrons in Ti and holes in PVK. Additionally, better performance can be expected by solving the bottleneck of poor conductivity of Ti, and giving optimized architectures of PVK layers filling the nanopores of porous triple layers. This work may have a great meaning for the further back-contacted perovskite SCs.

AUTHOR INFORMATION

Corresponding author

*****E-mail addresses: hayase@life.kyutech.ac.jp

ACKNOWLEDGMENT

This research was supported by Graduate School of Life Science and Systems Engineering, Kyushu Institute of Technology.

REFERENCES

(1) Xiao, Y.; Han, G.; Chang, Y.; Zhou, H.; Li, M.; Li, Y. An all-solid-state perovskite-sensitized solar cell based on the dual function polyaniline as the sensitizer and p-type hole-transporting material. *J. Power Sources* **2014**, *267*, 1-8.

(2) Sheikh, A. D.; Bera, A.; Haque, M. A.; Rakhi, R. B.; Gobbo, S. D.; Alshareef, H. N.; Wua, T. Atmospheric effects on the photovoltaic performance of hybrid perovskite solar cells. *Sol. Energ. Mat. Sol. C* **2015**, *137*, 6-14.

(3) Lang, L.; Yang, J.-H.; Liu, H.-R.; Xiang, H. J.; Gong, X. G. First-principles study on the electronic and optical properties of cubic ABX3 halide perovskites. *Phys. Lett. A*, **2014**, *378*, 290-293.

(4) Sakai, N.; Pathak, S.; Chen, H.-W.; Haghighirad, A. A.; Stranks, S. D.; Miyasak, T.; Snaith, H. J. The mechanism of toluene-assisted crystallization of organic–inorganic perovskites for highly efficient solar cells. *J. Mater. Chem. A* **2016**, *4*, 4464-4471.

(5) Nie, W.; Tsai, H.; Asadpour, R.; Blancon, J.-C.; Neukirch, A. J.; Gupta, G.; Crochet, J. J.; Chhowalla, M.; Tretiak, S.; Alam, M. A.; et al. High-efficiency solution-processed perovskite solar cells with millimeter-scale grains. *Science* **2015**, *347*, 522-525.

(6) Zhang, W.; Anaya, M.; Lozano, G.; Calvo, M. E.; Johnston, M.l B.; Míguez, H.; Snaith, H. J. Highly Efficient Perovskite Solar Cells with Tunable Structural Color. *Nano Lett.* **2015**, *15*, 1698-1702.

(7) Nagarjuna, P.; Narayanaswamy, K.; Swetha, T.; Hanumantha Rao, G.; Singh, S. P.; Sharma, G.D. CH3NH3PbI3 Perovskite Sensitized Solar Cells Using a D-A Copolymer as Hole Transport Material. *Electrochim. Acta* **2015**, *151*, 21-26.

(8) Savin, H.; Repo, P.; Gastrow, G. v.; Ortega, P.; Calle, E.; Garín, M.; Alcubilla, R.; Black silicon solar cells with interdigitated back-contacts achieve 22.1% efficiency. *Nat. Nanotechnol* **2015**, *10*, 624-628.

(9) Jeong, S.; McGehee, M. D.; Cui, Y. All-back-contact ultra-thin silicon nanocone solar cells with 13.7% power conversion efficiency. *Nat. Commun.* **2013**, *4*, 1-7.

(10) Fuke, N.; Fukui, A.; Komiya, R.; Islam, A.; Chiba, Y.; Yanagida, M.; Yamanaka, R.; Han, L. New Approach to Low-Cost Dye-Sensitized Solar Cells With Back Contact Electrodes. *Chem. Mater.* **2008**, *20*, 4974-4979.

(11) Nishio, Y.; Yamaguchi, T.; Yamguchi, T.; Nishio, K.; Hayase, S. Transparent conductive oxide-less dye-sensitized solar cells (TCO-less DSSC) with titanium nitride compact layer on back contact Ti metal mesh. *J. Appl. Electrochem.* **2016**, *46*, 551-557.

(12) Fu, D.; Zhang, X. L.; Barber, R. L; Bach, U.; Adv. Mater. Dye-Sensitized Back-Contact Solar Cells. **2010**, *22*, 4270-4274.

(13) Jumabekov, A. N.; Della Gaspera, E.; Xu, Z.-Q.; Chesman, A. S. R.; van Embden, J.; Bonke, S. A.; Bao, Q.; Vaka, D.; Bach, U. Back-Contacted Hybrid Organic-Inorganic Perovskite Solar Cells. *J. Mater. Chem. C* **2016**, *00*, 1-3.

(14) Mei, A.; Li, X.; Liu, L.; Ku, Z.; Liu, T.; Rong, Y.; Xu, M.; Hu, M.; Chen, J.; Yang, Y.; et al. A hole-conductor–free, fully printable mesoscopic perovskite solar cell with high stability. *Science* **2014**, *345*, 295-298.

(15) Sartale, S.D.; Ansari, A.A.; Rezvani, S.-J. Influence of Ti film thickness and oxidation temperature on TiO2 thin film formation via thermal oxidation of sputtered Ti film. *Mat. Sci. Semicon. Proc* **2013**, *16*, 2005-2012.

(16) El-Henawey, M. I.; Gebhardt, R. S.; El-Tonsy, M. M.; Chaudhary, S. Organic solvent vapor treatment of lead iodide layers in the two-step sequential deposition of CH3NH3PbI3-based perovskite solar cells. *J. Mater. Chem. A* **2016**, *4*, 1947-1952.

(17) Burschka, J.; Pellet, N.; Moon, S.-J.; Humphry-Baker, R.; Gao, P.; M. Nazeeruddin, K.; Gra¨tzel, M. Sequential deposition as a route to high-performance perovskite-sensitized solar cells. Nature **2013**, *499*, 316-319.

(18) Xie, W.; Chen, J.; Jiang, L.; Yang, P.; Sun, H.; Huang, N. Nanomesh of Cu fabricated by combining nanosphere lithography and high power pulsed magnetron sputtering and a preliminary study about its function. *Appl. Surf. Sci.* **2013**, *283*, 100-106.

(19) Torrisi, V.; Ruffino, F. Metal-Polymer Nanocomposites: (Co-)Evaporation/(Co)Sputtering Approaches and Electrical Properties. *Coatings* **2015**, *5*, 378-424.

(20) Xing, G.; Mathews, N.; Sun, S.; Lim, S. S.; Lam, Y. M.; Grätzel, M.; Mhaisalkar, S.; Sum, T. C. Long-Range Balanced Electron- and Hole-Transport Lengths in Organic-Inorganic CH3NH3PbI3. *Science* **2013**, *342*, 344-347.

(21) Stranks, S. D.; Eperon, G. E.; Grancini, G.; Menelaou, C.; M. Alcocer, J. P.; Leijtens, T.; Herz, L. M.; Petrozza, A.; Snaith, H. J. Electron-Hole Diffusion Lengths Exceeding 1 Micrometer in an Organometal Trihalide Perovskite Absorber. *Science* **2013**, *342*, 341-344.

(22) Dong, Q.; Fang, Y.; Shao, Y.; Mulligan, P.; Qiu, J.; Cao, L.; Huang, J. Electron-hole diffusion lengths > 175 μm in solution-grown CH3NH3PbI3 single crystals. *Science* **2015**, *347*, 967-970.

(23) Shi, D.; Adinolfi, V.; Comin, R.; Yuan, M.; Alarousu, E.; Buin, A.; Chen, Y.; Hoogland, S.; Rothenberger, A.; Katsiev, K.; et al. Low trap-state density and long carrier diffusion in organolead trihalide perovskite single crystals. *Science* **2015**, *347*, 519-522.

(24) Tripathi, N.; Yanagida, M.; Shirai, Y.; Masuda, T.; Han, L.; Miyano, K. Hysteresis-free and highly stable perovskite solar cells produced via a chlorine-mediated interdiffusion method. *J. Mater. Chem. A* **2015**, *3*, 12081-12088.

(25) Yoon, H.; Kang, S. M.; Lee, J.-K.; Choi, M. Hysteresis-free low-temperature-processed planar perovskite solar cells with 19.1% efficiency. *Energy Environ. Sci.* **2016**, *9*, 2262-2266.

TOC GRAPHIC

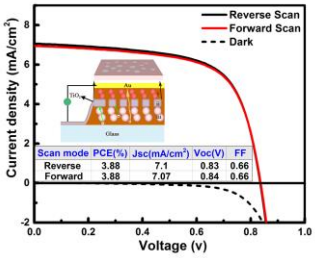
Reverse Scan
Forward Scan
Dark
Current density (mA/cm²)
Voltage (v)
Scan mode PCE(%) Jsc(mA/cm²) Voc(V) FF
Reverse 3.88 7.1 0.83 0.66
Forward 3.88 7.07 0.84 0.66